INTERNATIONAL
SOIL AND WATER
CONSERVATION RESEARCH

Investigation of time dependent development of soil structure and formation of macropore networks as affected by various precrop species

Sebastian K. Pagenkemper[1], Daniel Uteau Puschmann[2], Stephan Peth[3], and Rainer Horn[4]

Abstract

A well developed macropore network is advantageous in terms of transport processes regarding gas and water, as well as nutrient acquisition and root growth of crops. X-ray computed tomography provides a non-destructive method to visualize and quantify three-dimensional pore networks. Geometrical and morphological parameters of the complex pore system such as connectivity, tortuosity, porosity and pore surface area would be very useful for modeling and simulation of transport and exchange processes by providing quantitative data on relevant soil structural features and their modification by soil management.

The scope of this study was to analyze and quantify the development of soil structure in the subsoil depending on three different precrop species (alfalfa A, chicory C and fescue F), at three depths (45, 60 and 75 cm) and cultivation periods (1, 2 and 3 years). Furthermore, morphological (air-filled porosity θ_a, pore surface area) and geometrical (pore diameter, connectivity, continuity, tortuosity τ) parameters were gathered with X-ray CT and image analysis. From an experimental field trial (Germany) with a Haplic Luvisol as soil type samples were taken and investigated. Air-capacity (θ_a) was measured in the laboratory for the same cylinders and compared to the results derived by image analysis.

Air-capacity was highest for alfalfa (3 years, 75 cm). Tortuosity (τ) ranged between 1.3 and 4.38, while alfalfa (3 years) showed the highest value, which indicated structural development due to crack formation by enhanced root water uptake. Thus, an increase in accessible surface may improve water and nutrient supply for plants, whereas the high τ values may assume that oxygen supply is limited. It was found that the interaction of gas-diffusivity and the calculated parameters should be further investigated in terms of limitations to plant growth.

Key Words: Biological tillage, Image analysis, Batch processing, Subsoil structure, Dynamic development

1 Introduction

For the development of soil structure in agricultural crop land, a highly dynamic system has to be considered. While the topsoil layer generally is homogenized by ploughing (Garbout et al., 2013), the subsoil is strongly affected by compaction and deformation/shearing, but also flora and fauna that can have persistent effects on the three-dimensional pore geometry (Berli et al., 2004; Berisso et al., 2012; Dexter, 1997; Dexter et al., 2008; Gregory et al., 2010; Matthews et al., 2010). In negative terms, transmission functions such as gas and water transport are disturbed by compaction and shearing (Ball, 1988; Dexter, 2004; Horn et al., 1995; Lipiec and Hatano, 2003), while in positive terms, macro pores (Dörner et al., 2010; Matthews et al., 2010; Schäffer et al., 2007) and thus, respiration and crop growth are affected (Glinski and Stepniewski, 1985; Bartholomeus et al., 2008). In particular, gas transport is influenced by air-filled porosity (Arthur et al., 2012; Iversen et al., 2011;

[1] Post-Doctoral Fellow Dept. of Soil Science, Institute of Plant Nutrition and Soil Science, University of Kiel, Germany. Corresponding author: E-mail: s.pagenkemper@soils.uni-kiel.de

[2] Post-Doctoral Fellow, Dept. of Soil Science, Organic Agriculture Sciences, University of Kassel, Germany

[3] Professor, Dept. of Soil Science, Organic Agriculture Sciences, University of Kassel, Germany

[4] Professor, Dept. of Soil Science, Institute of Plant Nutrition and Soil Science, University of Kiel, Germany

Kristensen et al., 2010), but also connectivity, continuity and tortuosity (Eggleston and Peirce, 1995; Horgan, 1999; Kadžienė et al., 2011; Kristensen et al., 2010; Moldrup et al., 1998). Air-filled porosity, in addition to pore continuity and tortuosity, strongly influences the oxygen diffusion coefficient, which for water is 10.000 times larger compared to air. The oxygen diffusion coefficient is of major importance for plant growth and root survival. The surface area of pores is important for the storage and transport of nutrients and water (Hajnos et al., 2000), which is linked with the sorptive and ion exchange capacity (Ben-Dor and Banin, 1995). The root-soil contact area is important for root growth and nutrient acquisition (Schmidt et al., 2012).

With X-ray computed tomography (X-ray CT), it is possible to noninvasively visualize and quantify the structure of soils (Garbout et al., 2012; Naveed et al., 2013; Taina et al., 2008). Intact soil samples can be used for a direct estimation of soil structural attributes such as geometry, morphology, porosity, surface area, pore size distribution, pore shape, connectivity, continuity and tortuosity (Pagenkemper et al., 2013, 2014; Peth et al., 2008; Vogel et al., 2010). The calculated characteristics of pore networks can then be used for modeling and simulating state variables and flow parameters (air and hydraulic permeability, gas diffusion, preferential flows etc.), which are strongly correlated to the pore network characteristics (Moldrup et al., 2001; Kawamoto et al., 2006, Uteau et al., 2013). Further, the data can be used to predict saturated hydraulic conductivity using pore models and X-ray CT (Elliot et al., 2010), solute mass transfer effects regarding two-dimensional dual-permeability modeling (Gerke et al., 2013) or to assess the effects of soil structure on hydraulic behaviors by virtual soils (Schlüter et al., 2012).

It is well known that plants with specific root architectures develop characteristic structures, which in the case of tap rooted species are found to be dominated by vertically oriented biopores with lateral branches spreading into the surrounding bulk soil (Gregory, 2008; Kutschera at al., 2009). In turn, these structures may be explored by successive crops, which benefit from smaller mechanical resistance (Cresswell and Kirkegaard, 1995), improved nutrient and water supply (Kautz et al., 2012), and increased aeration (Anderson and Kemper, 1964), as they have a continuous connection into the topsoil layer via biopores (Kautz et al., 2010; Mitchell et al., 1995). To use plants as soil management utilities, one needs to know how far specific species in crop rotations can regenerate soil structure. Homorhizous species, fescue for example, will form widely branching root systems with adventitious and many fibrous roots (Schroetter et al., 2007) that can also penetrate greater depths via biopores and cracks (McKenzie et al., 2009). Allorhizous plants, such as alfalfa or chicory with their deep penetrating tap root systems, create vertical biopores (Hayes et al., 2010; Mitchell et al., 1995).

We hypothesized that the main contrast should be found between the allorhizous and homorhizous crops, meaning that different root architectures generate distinct pore networks. The main objective of this study was to investigate structure formation as a result of different root architectures (alfalfa, chicory and fescue) and the development of these different architectures over time using X-ray CT. Furthermore, morphological parameters (air-filled porosity, surface area, pore diameter) as well as geometrical parameters (connectivity, continuity and tortuosity) of the pore networks were extracted with image analysis. The investigations were conducted on samples from a field experiment (plot design), where the precrops have been continuously cultivated for one, two and three years. The calculated parameters were related to laboratory results measured for the same cylinders (air-capacity) to get an estimate of reliability of the values calculated with X-ray CT, for example volume and surface area of pores. Additionally, the findings were compared with measured diffusion coefficients and deducted tortuosity-indices obtained from slightly larger soil cores from the same field plots, which should validate the findings in terms of gas transport processes and emphasize the usability of the X-ray CT data for model approaches.

2 Material and methods

2.1 *Field description and soil sampling*

The field experiment was established in 2007 at the experimental station Klein Altendorf of the University of Bonn (50°37′ 9″ N lat; 6°59′ 29″ E long) and is characterized by a maritime climate with temperate humid conditions (9.3–9.6℃ mean annual temperature, 594–625 mm annual rainfall). The soil type is a Haplic Luvisol (hypereutric, siltic) developed from loess, characterized by an A-horizon (0–27 cm, silty loam), an E/B-horizon (27–41 cm, silty loam), a Bt-horizon (41–115, silty clay loam), a Bw-horizon (115–127 cm) and a silty loam, carbonate rich C-horizon (127 g kg^{-1} $CaCO_3$) beneath 127 cm (Table 1).

Table 1 **Description and basic properties of the reference soil profile**

Depth	Horizons	Texture				Bulk density	pH $CaCl_2$	$CaCO_3$	SOC
(cm)		Sand (%)	Silt (%)	Clay (%)	Textural class*	(g cm^{-3})		(g kg^{-1})	(g kg^{-1})
0–27	Ap	8	77	15	SiL	1.29	6.5	< 1	10.0
27–41	E/B	5	75	20	SiL	1.32	6.9	< 1	4.6
41–75	Bt1	4	69	27	SiCL	1.42	6.9	< 1	4.5
75–87	Bt2	4	66	30	SiCL	1.52	6.9	< 1	3.9
87–115	Bt3	5	70	25	SiL	1.52	7.1	< 1	2.5
115–127	Bw	5	72	23	SiL	1.46	7.3	< 1	2.6
127–140+	C	8	79	13	SiL	1.47	7.4	127	–

* IUSS Working Group WRB (2006).

Nine precrop treatments were investigated in a randomized complete block design with 60 m² size plots. The design included three crops: alfalfa (*Medicago sativa* L. subsp. *sativa*), chicory (*Cichorium intybus* L.) and fescue (*Festuca arundinacea* Schreb.); and three crop durations: one, two and three years of continuous cultivation. Seeding densities were 25 kg ha^{-1} for alfalfa, 5 kg ha^{-1} for chicory and 30 kg ha^{-1} for tall fescue (Gaiser et al., 2012). The precrops were sown in spring 2007, 2008, 2009 and 2010 respectively, after tillage by a mouldboard plough. Before the field trial started, different crops were cultivated in varying crop rotations between 1996 and 2007: fava bean (*Vicia faba* L.), sugar beet (*Beta vulgaris* subsp. vulgaris), summer barley (*Hordeum vulgare* L.), summer wheat (*Triticum aestivum* L.), triticale (×*Triticosecale* spp.), winter barley (*Hordeum vulgare* L.) and winter wheat (*Triticum aestivum* L). At the investigation site *Lumbricus terrestris* L. was the only deep-burrowing earthworm present, with an abundance of 10 to 40 individuals m^{-2} (Kautz et al., 2011). During the precrop phase, crops were cut four times a year and neither tillage nor fertilization was done.

In spring 2010 and 2011, Plexiglas® cylinders (5.1 cm in height and 4.4 cm in diameter) were used to extract intact soil cores. Seven replicates were taken from each treatment at 45, 60 and 75 cm depth in the soil profile by a manual stainless steel auger with randomized distribution of the replicates over an area of approximately 1–2 m^2 at each depth. The number of samples (n) ranged between 7 and 14.

2.2 *Gas diffusion measurements*

To prepare the samples for the measurements, soil cores were saturated from beneath, then drained and weighted at a matric potential of –150 hPa using ceramic plates to estimate air-filled porosity (Ball et al., 1988). The estimation of relative gas diffusion coefficients and the deduction of tortuosity-indices were conducted for a separate set of soil samples, described in detail in Uteau et al. (2013). Soil cores (10 cm diameter, 10 cm height) were saturated from beneath and drained at a matric potential of –60 hPa to quantify air-filled porosity and to conduct measurements.

2.3 *Acquisition and processing of data with X-ray CT*

231 soil cores were scanned with a *phoenix nanotom®s* (Phoenix-X-Ray, GE-Sensing and Inspection Technologies GmbH, Wunstorf, Germany). The scan specifications were: 105 keV energy, 225 µA current with a 0.1 mm copper filter between the X-ray source and the sample. The scans were conducted after the soil samples were drained to –150 hPa matric potential. By draining the samples, X-ray scattering which often occurs at high water content was reduced, thus improving image quality. Because the samples did not shrink during drainage it could be assumed that the soil structure was still rigid at –150 hPa.

Reconstruction was done with *datos|x* (GE-Sensing and Technologies GmbH, Wunstorf, Germany), using a modified Feldkamp backprojection algorithm (Feldkamp et al., 1984). The achieved resolution for each voxel was 51.31 µm. The air-filled porosity calculated with X-ray CT was determined considering the smallest pore diameter detected, which was 102.62 µm. Before image analysis, a region of interest (ROI) was chosen from the scanned cylinders. The ROI size was chosen to exclude physical disturbances at the top and bottom and sides of samples. The ROI size (54 cm^3) was equal for all samples and subsequently was used for image analysis.

2.4 *Image analysis*

The reconstructed data was processed with the *3DMA-Rock* software developed by Lindquist et al. (2000), which is explained below in paragraphs *'2.4.1'*and *'2.4.2'*. For the simultaneous processing of multiple soil samples (7 samples = 1 cycle), a batch system was used. The duration for one cycle was approx. 2–3 hours with the following cluster server setup: AMD Opteron 2220 SE (2.8 GHz, 4 cores), 8GB RAM (Registered DDR2 667/PC5400). To organize the image analysis results, a database (MySQL) was used. Queries from this database could directly be analyzed with the *R-package* (R Development Core Team, 2011). 3D rendering and visualization of pore networks was done with *VGStudio Max 2.0* (Volume Graphics GmbH, Heidelberg, Germany).

2.4.1 Image segmentation

An image segmentation algorithm was applied (Pagenkemper et al., 2013, 2014) to transform a gray scale image that illustrates the local distribution of material densities into a bimodal image displaying only the extracted pore network (white) and the surrounding soil matrix (black). A local adaptive thresholding algorithm was used in combination with two-pass indicator kriging (Oh and Lindquist, 1999). Two threshold values (T_0 and T_1) determine sections in a histogram, where the section below T_0 and the section above T_1 contain the gray values that can certainly be assigned to either the pore space or soil matrix voxel fraction, respectively. The voxels in the section in-between both thresholds, were assigned to either one of the two fractions due to indicator kriging. For the selection of the threshold parameters T_0 and T_1, a bimodal histogram was prepared that contained the soil matrix peak data from the whole region of interest (ROI) as well as the pore space peak data that consists of average gray value frequencies from the sub-ROI data (randomized selected regions just around visible porous structures to clearly distinguish a pore and a soil matrix peak in the histogram). With the curve fitting program *FitYK* (Wojdyr, 2010) the parameters for Gaussian distributions of the pore and soil matrix peaks were estimated, which were used to estimate T_0 and T_1. The estimated values for T_0 and T_1 were subsequently used for image segmentation.

2.4.2 Calculation of network parameters

With the algorithms for segmented and medial axis data, provided by *3DMA-Rock* (Lindquist et al., 1995), morphological (porosity, pore surface area) and geometrical (connectivity, continuity, tortuosity) parameters of the investigated pore network were calculated (Pagenkemper et al., 2013, 2014). The algorithms for processing of the segmented data were used to calculate:

(i) The porosity that depends on voxel resolution and voxel count of the resolved pore space.

(ii) The pore surface area, which is calculated via surface triangulation.

With the medial axis algorithm a discrete view of the pores was generated, which consisted of medial axis voxels that illustrate the centered 'backbone' of the detected pores. This provided a simplified representation of the geometry of pores and was used to calculate:

(i) The pore diameter, which was calculated with a burn algorithm that determines the radius of a pore channel (in counts of voxels) and is interpreted by the largest ball centered at the medial axis and just fits inside the pore space.

(ii) The geometrical tortuosity (τ), which was characterized as the ratio of the curved path length and the Euclidean distance of the path connected between two parallel planes. It was expressed as a number $\geqslant 1$. A straight path was denoted with $\tau = 1$, whereas increasing values denoted an increasing tortuosity.

(iii) The continuity of the pore network was denoted as the number of paths with a continuous connection between accessible pores at the top and bottom side of the investigated samples.

(iv) The connectivity of the pore network was referred to as the relative value of interconnected porosity of the total porosity.

Because the medial axis algorithm creates different types of paths, we focused on two types of paths that are most important for transport processes in porous media (other paths have been removed during a trimming routine): Vertical continuous pores are represented by multiple long interconnected branch-branch paths. Lateral pores that are distributed in the soil matrix are described by shorter single branch-leaf paths that are connected to the vertical branch-branch paths (Lindquist et al., 1995).

2.5 *Statistical analysis*

Effects of precrop species (alfalfa, chicory and fescue), depth (45, 60 and 75 cm) and crop duration (one,

two and three years cultivation) on air-filled porosity and pore surface area were tested with ANOVA, coupled with a multiple contrast test for independent variables. Results were classified as statistically significant at $p<0.05$.

3 Results and discussion

3.1 *Air-filled porosity calculated with X-ray CT*

The tomograms in Fig. 1 show vertical cross sections from alfalfa, chicory and fescue in 45 and 75 cm depth for one, two and three years of cultivation. The visual assessment revealed that the structural formation differs depending on precrop, time and depth. Alfalfa apparently produced distinct effects in terms of formation of macropores followed by chicory and fescue in the sequence from year one to three. This is more pronounced by the results of quantitative image analysis of the replicates.

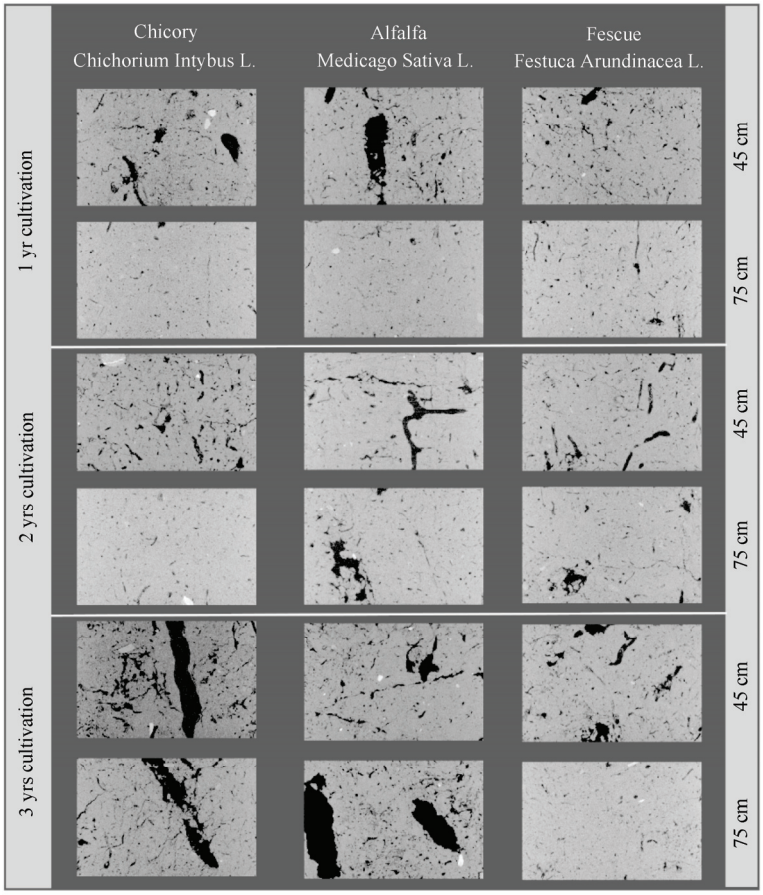

Fig.1 The X-ray CT tomograms show vertical cross sections of soil samples from chicory, alfalfa and fescue treatments after one, two and three years cultivation from 45 and 75 cm depth in the soil profile illustrating pore architecture development in dependency of precrop, time and depth

The air-filled porosity (θ_a) calculated from X-ray CT data, showed distinct differences between the three precrops as a result of development with time and depth (Fig. 2), which was denoted by structure formation illustrated in the two-dimensional tomograms (Fig. 1). In general θ_a can be classified as 'low/medium air capacity' (Ad-Hoc-AG Boden, 2005). Fescue showed only little structural change with time, mostly restricted to 45 cm, whereas alfalfa and chicory developed well in the upper subsoil after two years of cultivation. Especially for alfalfa after three years cultivation, a significant increase of θ_a from 45 to 60 and 75 cm depth was found, while the cultivation periods resulted in a significant increase of the air-filled porosity for alfalfa (all depths) and chicory (60 cm) after three years cultivation.

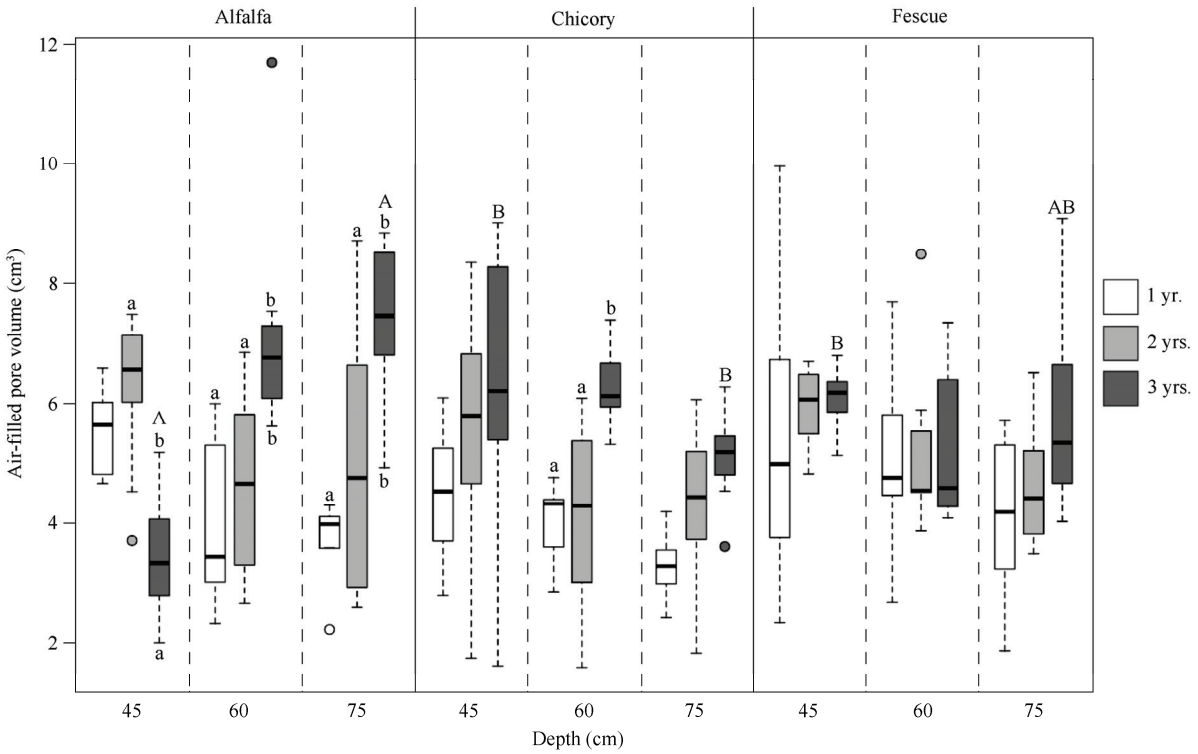

Fig. 2 X-ray CT determined air-filled porosity for fescue, alfalfa and chicory, for 45, 60 and 75 cm depth and after 1, 2 and 3 years cultivation
[The letters indicate the results of post-hoc-test for the comparisons of the arithmetic means: Significant differences (level of significance $p<0.05$) are shown for the comparison of alfalfa, chicory and fescue (upper capital letters). The cultivation periods, respectively 1, 2 and 3 years, as upper letters. The depths, respectively 45, 60 and 75 cm, as lower letters. Number of samples (n) = 7.]

Overall, the factors duration, depth and precrop (in that order) have a significant influence on θ_a, there is also a strong influence of duration and depth. Uteau et al. (2013) found for the same study site that processes of enhancement in air-filled porosity need at least three years to show significant effects and that for fescue the pore formation was restricted to 50 cm depth, whereas for alfalfa great enhancements were found at 60–90 cm and for chicory up to 90 cm of depth. Considering that the pore formation may be seen as a result of root activity, Mitchell et al. (1995) and Meek et al. (1989) stated that for alfalfa, water flow processes should show enhancements after a growth period of more than two years. Alfalfa roots are suggested to be fully developed after three years (Pietola and Smucker, 1995; Rasse et al., 2000), which was found here and was also shown by Uteau et al. (2013). Strong influences can be found at depths greater than 60 cm. For alfalfa, decreasing θ_a after two years from 45–75 cm depth were found compared with increasing θ_a from 45–75 cm depth after three years. Thus, it can be assumed that further production cycles can also result in more distinct increases of θ_a in shallower depths by structure formation.

3.2 *Pore surface area calculated with X-ray CT*

In Fig. 3, the calculated pore surface areas for the three crops, durations and depths are illustrated. For alfalfa significant differences were found from 45–75 cm depth after three years with an increasing surface area. This was also found between alfalfa and the two other crops at 45 cm depth after three years cultivation. The pore surface area is correlated with the pore geometry: Elongated vertically oriented biopores created by taproot systems or earthworms are linked with a larger connected pore volume and relatively lower pore surfaces compared to more heterogeneous oriented macropores, created by shallow root systems that result in smaller pore volumes and relatively larger surface areas. For the example of alfalfa, this may indicate that newly developed surfaces increased accessible surface area by structure formation, which was also found to a lesser extent for chicory. The root-soil interface is essential for water and nutrient acquisition by plant roots and, for example, can be influenced

by an increase of root hair density and length, which positively affects phosphorous acquisition of wheat and barley cultivars (Gahoonia et al., 1997). But more importantly, soil structure influences root-soil contact by aggregation, soil compaction and pore diameters (Tinker, 1976; Nye, 1994). Bastardie et al. (2005) reported that pore walls, which are connected with the soil surface, are considered to extend the surface inside the soil profile. Thus, it can be assumed that this extension is enhanced by lateral pores and cracks distributed in the bulk soil, as was found for alfalfa and chicory.

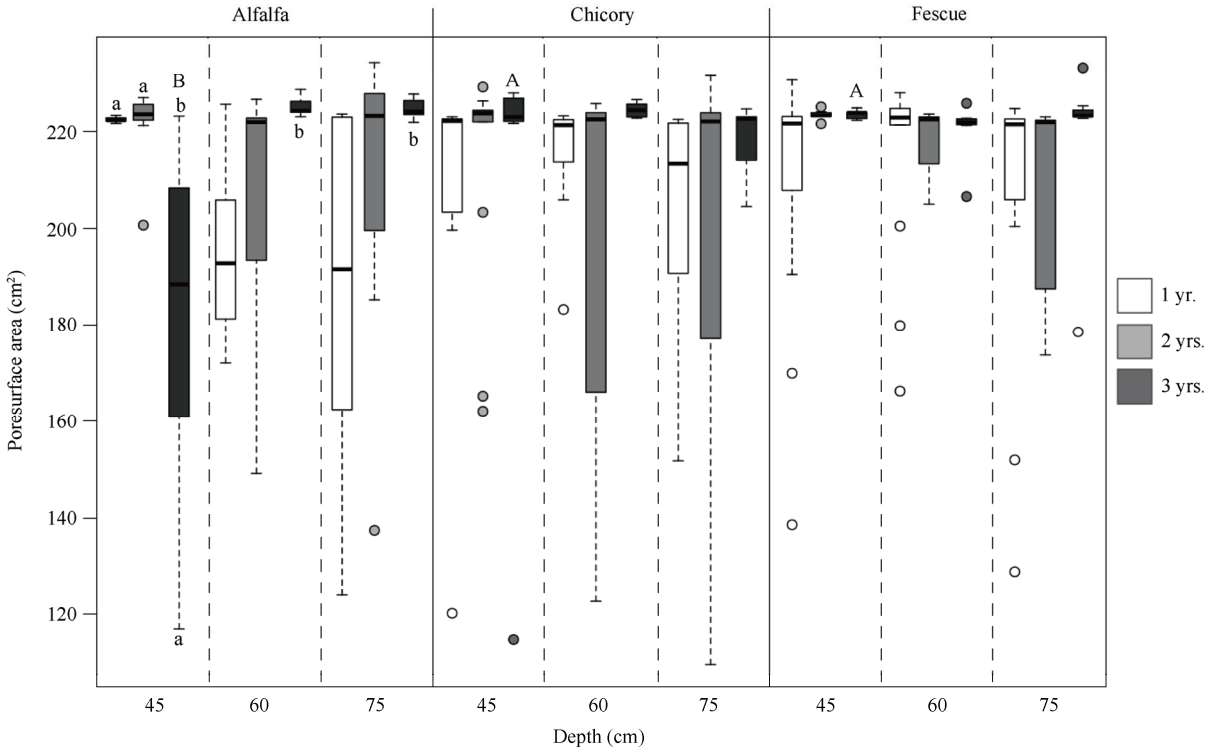

Fig. 3 X-ray CT determined pore surface area for fescue, alfalfa and chicory, in 45, 60 and 75 cm depth and after 1, 2 and 3 years cultivation
[The letters indicate the results of post-hoc-test for the comparisons of the arithmetic means: Significant differences (level of significance $p<0.05$) are shown for the comparison of alfalfa, chicory and fescue (upper capital letters). The cultivation periods, respectively 1, 2 and 3 years, as upper letters. The depths, respectively 45, 60 and 75 cm, as lower letters. Number of samples (n) = 7.]

The enhancements of pore surface area by newly formed shrinkage cracks due to root water uptake were identified with X-ray CT tomograms (Fig. 4) and emphasize the quantitative results of an increased air-filled porosity and surface area found for alfalfa and chicory as a result of cultivation time.

Still, those effects on porosity and pore surface as a result of root induced structure formation should be investigated, which may be further supported by this work and algorithms for segmentation of roots (Kaestner et al., 2006, Mairhofer et al., 2013, 2012; Tracy et al., 2010).

3.3 *Relation between θ_a values from laboratory and X-ray CT data*

X-ray CT and image analysis were introduced as tools for the estimation of morphological parameters, such as porosity and surface area. Compared to the surface area of pores, the porosity of soils can easily be estimated under laboratory conditions and provides an estimate of air-capacity. As the validation of the data gathered with X-ray CT is of importance for a potential use in model approaches, the air-filled porosity calculated with X-ray computed tomography was compared with gravimetrically estimated θ_a values from the same soil cores. θ_a showed a good correlation (Fig. 5) with the laboratory data. This was also tested with intact soil cores from the same study site with a larger sample volume (data not shown), where a similar correlation was found. Because the applied algorithms for the calculation of surface area in the example relate to the same data used for porosity

calculations, we assume that the results should also be valid. This may provide improvements in simplicity and time needed to estimate pore surface area, because this parameter is mostly estimated by using computer models (Ersahin et al., 2006) or by the Brunauer Emmet Teller (BET) method (Dogan et al., 2006).

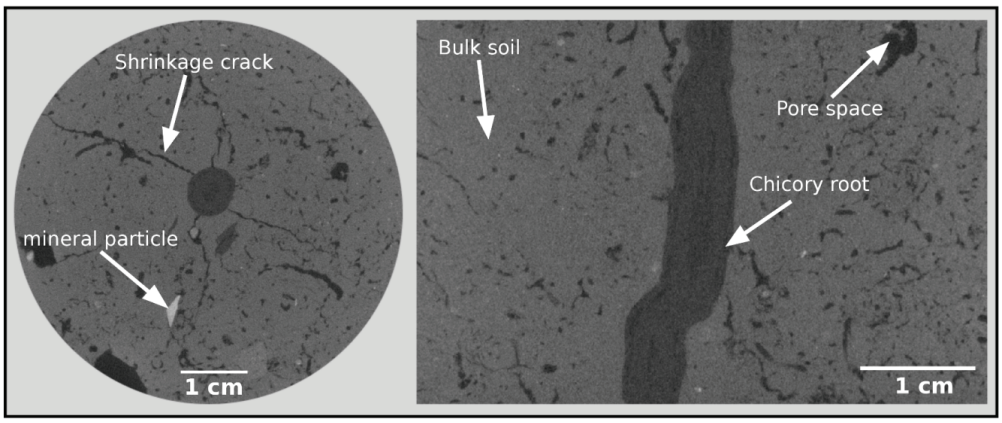

Fig. 4 Illustration of X-ray CT tomograms from a chicory sample (45 cm depth, 3 years cultivation) [Cross-section (left) and longitudinal-section (right) showing a biopore colonized by a chicory root. Shrinkage cracks (left) indicate structure formation by root water uptake.]

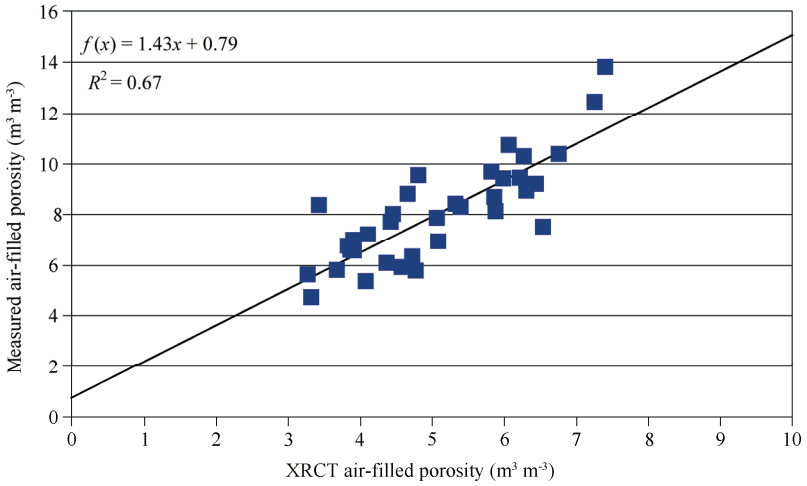

Fig. 5 Correlation of gravimetrically measured and X-ray CT determined air-filled porosity (squares) from the same cylinders, illustrated as arithmetic means for all treatments (alfalfa, chicory and fescue) and depths (45, 60 and 75 cm) [Number of samples (*n*) = 7.]

3.4 *Network parameters*

Transport processes in soils strongly depend on the spatial distribution of soil geometrical properties. Considering the two-dimensional tomograms (Fig. 1) it is not possible, to assess functions quantitatively or even visually. Fig. 6 shows three-dimensional reconstructions of pore networks derived from alfalfa, chicory and fescue. It is revealed that soil structure consists of a very complex arrangement of pores inside a network.

Additionally, features of those networks are revealed and indicate distinct differences between developed structures under the three precrops. Predominantly, biopores (vertical oriented) were found for the alfalfa and chicory treatment, which provides an estimate for possible effects on preferential transport processes.

3.4.1 Pore diameters

The pore diameters (Fig. 7) showed varying results but no distinct differences neither for the precrops nor depth and cultivation time. The greatest pore diameter overall was found for fescue 60 cm depth after two and three years cultivation, followed by alfalfa 60 cm after two years and 75 cm after 3 years, whereas chicory

showed maximum pore diameters at 45 cm (after one year cultivation) and 60 cm depth (after two years cultivation). Fescue showed no clear trends of development of specific pore diameters, as it was also found for porosity and surface area. In contrast, alfalfa showed a trend in formation of larger pore diameters with depth after three years, but the question remains open, in how far a decrease of pore diameters at 45 and 60 cm depth from the 2nd to the 3rd year could be explained.

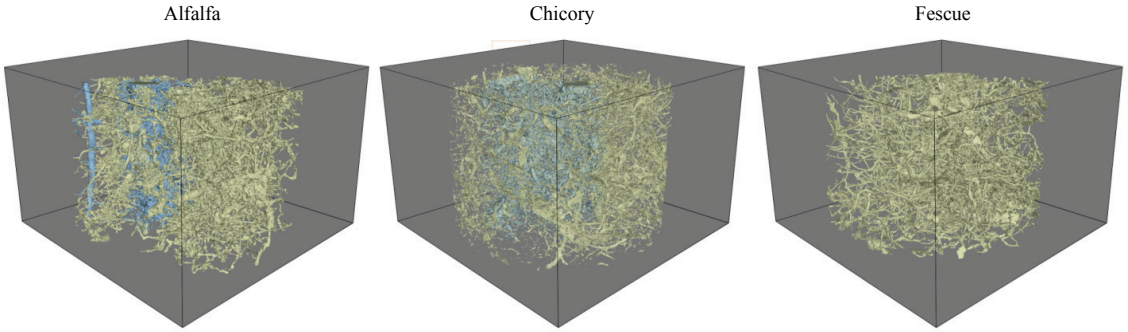

Fig. 6 Three-dimensional illustrations of the pore network reconstructions for alfalfa, chicory and fescue at 75 cm depth after three years cultivation (For alfalfa and chicory distinct biopores colored in blue with connections to pores in the bulk soil were found. The dimensions are: 5 cm×5 cm×4 cm at ~50µm voxel resolution.)

Obviously, the pore diameters reflected that not only plant roots, but also soil fauna (e.g., earthworms) affect the formation of larger pore diameters for fescue as shown in Fig. 7. Thus it can be assumed that the pore networks derived by the precrops are influenced by overlaying and integrated networks of earthworms in the field. The extensive reuse of biopores was explained in Pagenkemper et al. (2013, 2014). It was found that biopore networks at a large scale must have been influenced by plant roots and earthworms, as no distinct differences in pore formation were stated as a result only of root growth.

3.4.2 Tortuosity

Pore network parameters such as connectivity and tortuosity can directly be quantified with X-ray CT for three-dimensional intact sample volumes (Mooney, 2002), which is an advantage compared to the indirect estimations via diffusion-based analysis in example (Moldrup et al., 2001). The geometrical tortuosities (τ), which can be applied for modeling gas diffusion processes, were not significantly different between the treatments. For all treatments a variation in tortuosity of 1.3–4.3 (minimum and maximum calculated porosities included, not shown in the table) were found (Table 2). The values for tortuosity calculated with X-ray CT showed differences to the tortuosity (as power-law exponent) described by Marshall (1959) and Millington (1959), which were 1.33 and 1.5 respectively. Buckingham (1904) also used a constant value of 2.0 for the power-law model. Deepagoda et al. (2010) described that tortuosity strongly depends on soil water matric potential (given by pF) and showed variations of the tortuosity factor, as it monotonically decreased with increasing pF (minimum at pF 3) due to draining of inter-aggregate pores. Between pF 1.8 and 2.5 (–60 to –300 hPa), they found tortuosity values between 1.7 and 2.2 for intact, aggregated soils, which is in agreement with the tortuosity values derived from our X-ray CT calculations.

Table 2 Tortuosities calculated via X-ray CT and image analysis (τ) and tortuosity-indices (τ_i) adapted from Uteau et al. (2013) for fescue, alfalfa and chicory after one, two and three years of cultivation

Method	Duration	Alfalfa	Chicory	Fescue
τ	1	1.98 (0.22)	1.97 (0.18)	2.04 (0.14)
	2	2.04 (0.16)	2.12 (0.28)	1.98 (0.15)
	3	2.14 (0.45)	1.94 (0.13)	1.98 (0.16)
τ_i	1	1.59 (0.17)	1.52 (0.22)	1.49 (0.17)
	2	1.61 (0.28)	1.40 (0.13)	1.50 (0.20)
	3	1.85 (0.14)	1.25 (0.20)	1.46 (0.26)

Note: Values are expressed as median values and standard deviation in brackets. τ: n=7. Fescue 1, Alfalfa 2 and Chicory 2 with n=14. τ_i: n=6 for all treatments.

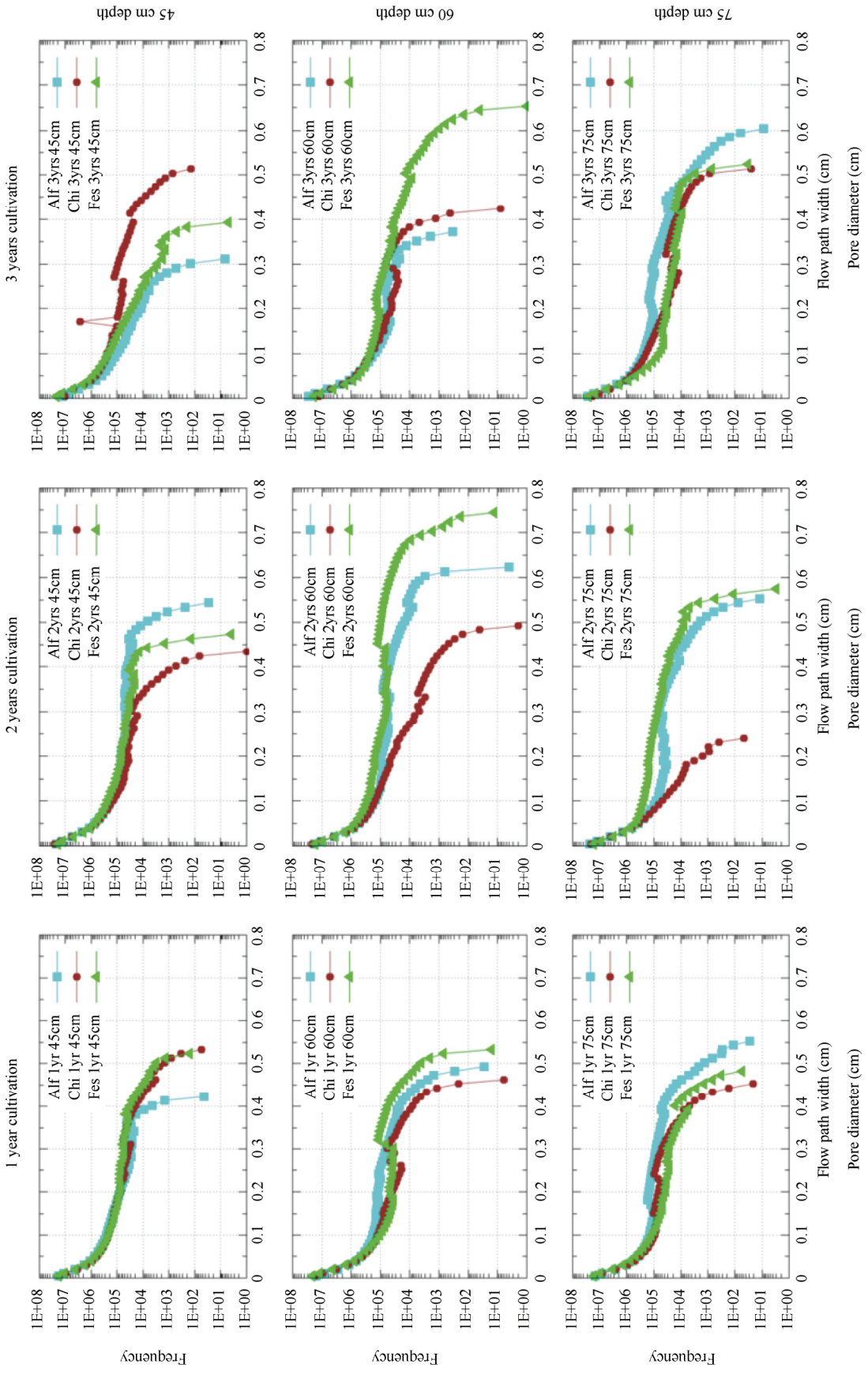

Fig. 7 Calculated pore diameters and frequency for the three precrops (alfalfa=square, chicory=circle, fescue=triangle) after one, two and three years cultivation (from left to right) in 45, 60 and 75 cm depth (from top to bottom) (*n*=7)

The τ values were compared to tortuosity-indices (τ_i) that were deducted from gas diffusion measurements for soil samples from the same study area that continuously showed lower values (Table 2). However, the overall trends for higher tortuosities with increasing depth for alfalfa in example were similar to the τ_i values while compared to alfalfa, fescue showed decreasing tortuosities with increasing depths. Considering the definition of tortuosity (given in the materials and methods section), the detected pores were found to be extended in length by a factor ranging from 0.3–3.3. This gives the assumption that plant growth may be affected by the length of pathways (tortuosity value) and the oxygen supply to the rhizosphere. However, tortuosity as a single parameter is not qualified for such statements and therefore gas diffusivity should also be considered (section *'3.5.4 Gas diffusivity'*).

3.4.3 Continuity and connectivity

Referring to the three-dimensional pore network reconstructions (Fig. 6), it is obvious that continuity and connectivity are related to the spatial orientation of pores and their interconnections. The reconstructed pore network of alfalfa for example, consisted of some single voids but also a larger interconnected network that is linked with the two biopores. Considering the air-filled porosities (Fig. 2), the connectivity value shown in Fig. 8 describes the porosity share of the interconnected network compared to the total air-filled porosity. Inside this alfalfa network, 1.94 continuous paths per cm³ were detected [as median value with a number of samples (n) = 7] between the top and bottom of the sample boundaries (Table 3), which was observed to be the lowest values compared to the other treatments. Alfalfa showed trends of increasing continuity with increasing cultivation duration for 60 and 75 cm depth, which were observed for chicory in 45 and 75 cm depth, for fescue in 75 cm only, and a decreasing trend in 45 cm alfalfa. While chicory and fescue showed decreasing trends of continuity from 45–75 cm for the same years, alfalfa was observed to show an increasing trend for the third year. As there were no comparable results found in the literature, these values still have to be tested for significance.

Table 3 Calculated continuity values for alfalfa and chicory after one, two and three years of cultivation. Continuity is expressed as continuous path per cm³ between the top and bottom borders of a sample

Duration	Alfalfa	Chicory	Fescue
1	2.35 (1.97)	2.83 (1.27)	2.41 (2.64)
2	3.17 (3.52)	2.70 (9.17)	4.13 (1.87)
3	1.94 (2.03)	3.57 (2.86)	3.30 (3.85)

Note: Values are expressed as median values and standard deviation in brackets. Number of samples (n) = 7; For Alfalfa 2 years , Chicory 2 years and Fescue 1 year the number of asmples (*n*) = 14.

The calculated continuity and connectivity values indicated that the connected pore networks should positively contribute to the subsoil aeration by mass flow. This was considered in the following section, as the findings that have been presented so far were related to gas diffusion measurements. Still, an important requirement for the functionality of those pores for transport processes in soils is that these described networks have a continuous connection at the pedon scale. This emphasizes the necessity of continuous, vertical biopores at a larger scale that are connected to the atmosphere.

3.4.4 Gas diffusivity

Considering that oxygen diffusion rate correlates with plant growth (Paul and Lee, 1976), low gas diffusivities that are linked with tortuosity, respectively the length of pathways to or from the rhizosphere, can affect metabolic processes in plants due to oxygen shortage (Allaire et al., 1996; Glinski and Stepniewski, 1985). It can be assumed that increasing tortuosity values may lead to oxygen shortages in the rhizosphere. For alfalfa an increasing trend for tortuosity was observed from the 1st to the 3rd year of cultivation. Still, alfalfa also showed increasing porosities as well as the highest porosity in 75 cm after three years cultivation, while Uteau et al. (2013) found that the oxygen diffusion for alfalfa also showed an increase from 45–75 cm after three years cultivation (Fig. 9). It can be assumed that tortuosity as a single value can qualitatively describe the impact on functions in the soil. Since other parameters are involved (e.g., air-filled porosity), high porosity values for alfalfa may compensate for effects that occurred as a result of tortuosity. Iversen et al. (2011) stated that gas transport into the subsoil is mainly influenced by air-filled porosity, which also can increase growth of secondary roots that is correlated to an increase of θ_a (Liang et al., 1996). This is true for the example of alfalfa, as the

increase in tortuosity due to the high porosity may not only be a barrier, but also an indicator for structure development by root water uptake and lateral root growth, perhaps resulting in an increase of accessible surface area as was shown previously. In turn. these surfaces provide a possible supply of plant roots with water and nutrients.

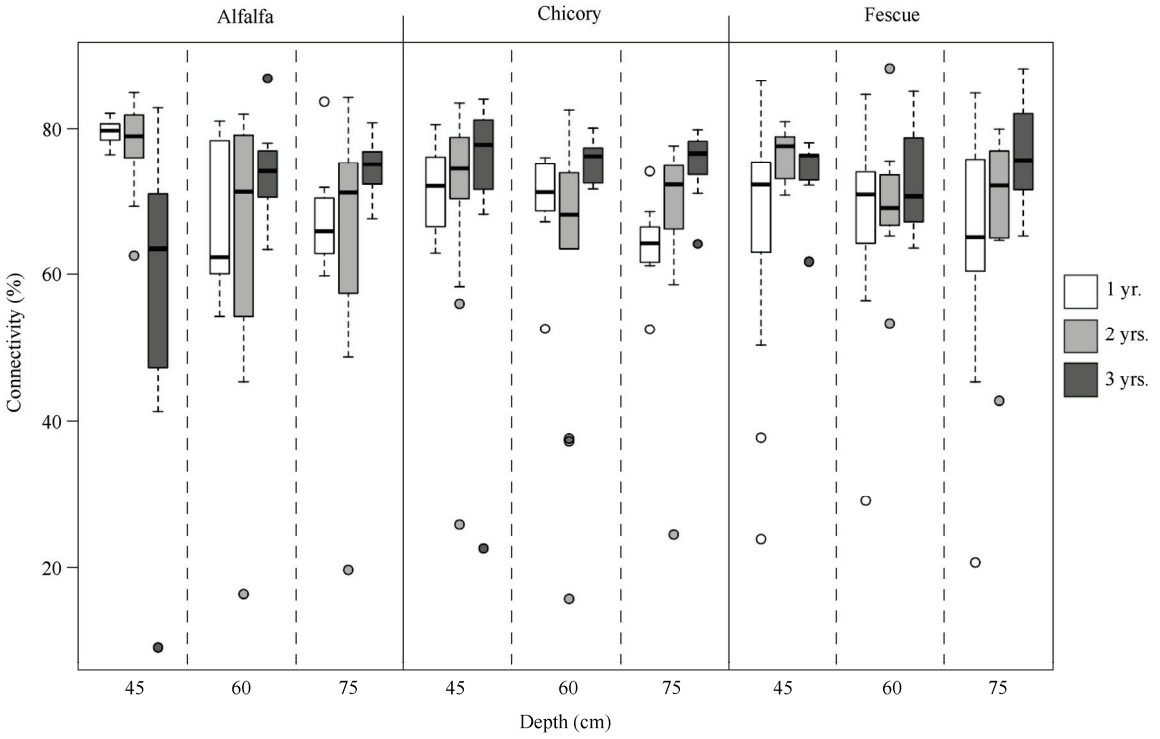

Fig. 8 X-ray CT determined connectivity for fescue, alfalfa and chicory, in (45, 60 and 75 cm depth and after 1, 2 and 3 year cultivation (*n*=7)

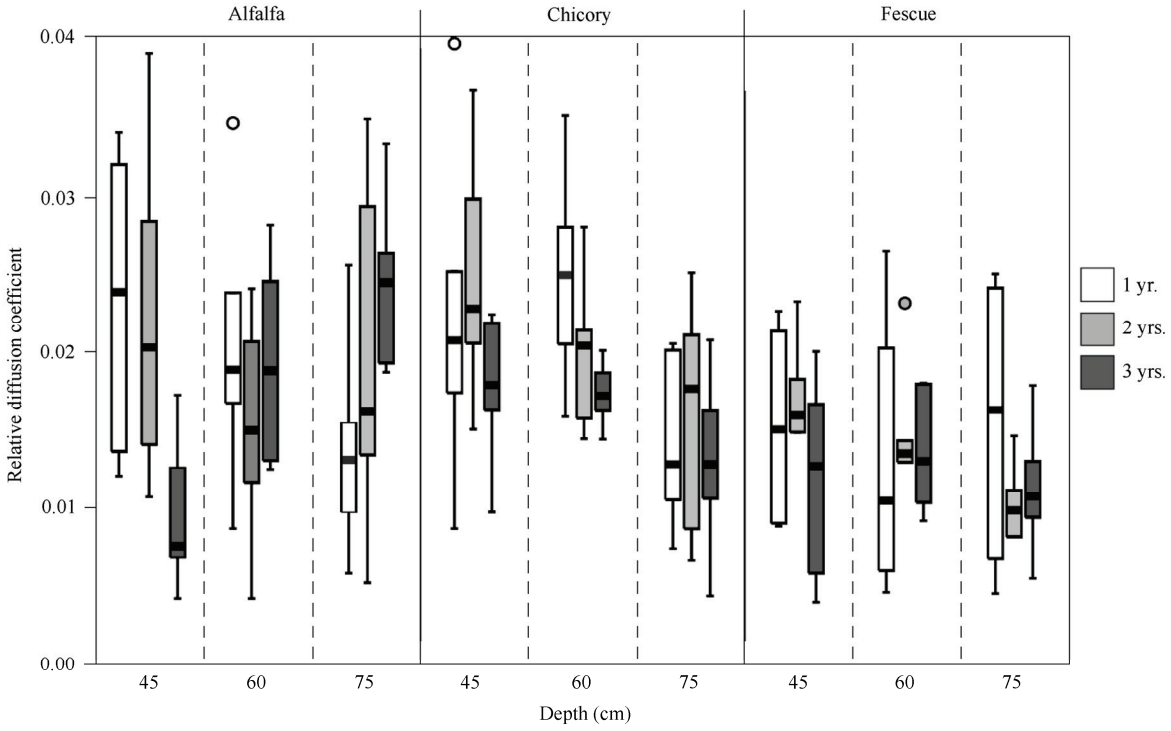

Fig. 9 Relative diffusion coefficients for three crops, three depths at a matric potential of –60 hPa [*n*=6. Adapted from Uteau et al. (2013)]

In particular, continuity and tortuosity have been mentioned as perhaps more important than volume or number of macropores for movement processes in soil (Ball, 1988; Allaire et al., 2002; Allaire-Leung et al., 2000a, 2000b), because diffusion inside macropores depends mainly on the spatial arrangement of macropores (Capowiez et al., 2006). However, as a certain continuity and connectivity of the pores inside a network was found, the question is how far the interaction of those parameters has limiting effects on plant growth due to their effects on oxygen diffusion. This is a question that should be considered for future research.

4 Conclusions

With the data presented here, the main hypothesis could be answered: Morphological and geometrical parameters derived by X-ray CT and image analysis were affected by the investigated precrops and their development with time and depth. With respect to the complex tap root system of alfalfa and the crack formation induced by root water uptake, higher tortuosities with time and depth coupled with an increase of air-filled porosity indicated structure development by swelling/shrinking. For fescue, a lower tortuosity coupled with decreasing air-filled porosity with depth may indicate the characteristic effects of shallow root architectures. With an increasing air-filled porosity with time and the observed maximum pore diameters, it may be assumed that earthworms strongly affected porosity and diameter of pores but with less tortuous pores. Alfalfa was observed to generate differences in general after a cultivation period of three years, whereas in terms of bioturbation and structure development much longer production cycles can be suggested, to generate more distinct effects pronounced by this root architecture. With the purpose to relate the findings with measurements from the laboratory, a good correlation was found, whereas it can be assumed that also other directly calculated parameters are reliable. With the relation of morphological and network properties to gas-diffusivity, there is a need for further research, because it is uncertain how much the interaction of those parameters may influence viable functions for plant growth.

Acknowledgements

This study was supported by the German Research Foundation (Deutsche Forschungsgemeinschaft DFG) within the framework of the research unit DFG‐FOR 1320. Details of the field trial potentially open for external researchers: www.for1320.uni‐bonn.de.

References

Ad-Hoc-AG Boden.(2005). Bodenkundliche Kartieranleitung: Ad-hoc-ARBEITSGRUPPE BODEN der Geologischen Landesämter und der Bundesanstalt für Geowissenschaften und Rohstoffe der Bundesrepublik Deutschland. Schweizerbart'Sche Verlagsbuchhandlung.

Allaire-Leung, S. E., Gupta, S. C., & Moncrief, J. F. (2000a). Water and solute movement in soil as influenced by macropore characteristics: 1. Macropore continuity. *Journal of Contaminant Hydrology*, *41*(3), 283-301.

Allaire-Leung, S. E., Gupta, S. C., & Moncrief, J. F. (2000). Water and solute movement in soil as influenced by macropore characteristics: 2. Macropore tortuosity. *Journal of contaminant hydrology*, *41*(3), 303-315.

Allaire, S. E., Caron, J., Duchesne, I., Parent, L. É., & Rioux, J. A. (1996). Air-filled porosity, gas relative diffusivity, and tortuosity: indices of Prunus× Cistena sp. growth in peat substrates. *Journal of the American Society for Horticultural Science*, *121*(2), 236-242.

Allaire, S. E., Gupta, S. C., Nieber, J., & Moncrief, J. F. (2002). Role of macropore continuity and tortuosity on solute transport in soils: 2. Interactions with model assumptions for macropore description. *Journal of contaminant hydrology*, *58*(3), 283-298.

Anderson, W. B., & Kemper, W. D. (1964). Corn Growth as Affected by Aggregate Stability, Soil Tempearture, and Soil Moisture. *Agronomy Journal*, *56*(5), 453-456.

Arthur, E., Moldrup, P., Schjønning, P., & de Jonge, L. W. (2012). Linking particle and pore size distribution paramters to soil gas transport properties. *Soil Science Society of America Journal*, *76*(1), 18-27.

Ball, B. C., O'sullivan, M. F., & Hunter, R. (1988). Gas diffusion, fluid flow and derived pore continuity indices in relation to vehicle traffic and tillage. *Journal of Soil Science*, *39*(3), 327-339.

Bartholomeus, R. P., Witte, J. P. M., van Bodegom, P. M., van Dam, J. C., & Aerts, R. (2008). Critical soil conditions for oxygen stress to plant roots: Substituting the Feddes-function by a process-based model. *Journal of Hydrology*, *360*(1), 147-165.

Bastardie, F., Ruy, S., & Cluzeau, D. (2005). Assessment of earthworm contribution to soil hydrology: a laboratory method to

measure water diffusion through burrow walls. *Biology and fertility of soils*, *41*(2), 124-128.

Ben-Dor, E., & Banin, A. (1995). Near-infrared analysis as a rapid method to simultaneously evaluate several soil properties. *Soil Science Society of America Journal*, *59*(2), 364-372.

Berisso, F. E., Schjønning, P., Keller, T., Lamandé, M., Etana, A., de Jonge, L. W., ... & Forkman, J. (2012). Persistent effects of subsoil compaction on pore size distribution and gas transport in a loamy soil. *Soil and Tillage Research*, *122*, 42-51.

Berli, M., Kulli, B., Attinger, W., Keller, M., Leuenberger, J., Flühler, H., ... & Schulin, R. (2004). Compaction of agricultural and forest subsoils by tracked heavy construction machinery. *Soil and Tillage Research*, *75*(1), 37-52.

Buckingham, E. (1904). Contributions to our knowledge of the aeration of soils.Bur. Soil Bull. 25. (U.S. Gov. Print. Office: Washington, DC).

Capowiez, Y., Bastardie, F., & Costagliola, G. (2006). Sublethal effects of imidacloprid on the burrowing behaviour of two earthworm species: modifications of the 3D burrow systems in artificial cores and consequences on gas diffusion in soil. *Soil Biology and Biochemistry*, *38*(2), 285-293.

Cresswell, H. P., & Kirkegaard, J. A. (1995). Subsoil amelioration by plant-roots—the process and the evidence. *Soil Research*, *33*(2), 221-239.

Deepagoda, T. K. K. C., Moldrup, P., Yoshikawa, S., Kawamoto, K., Komatsu, T., & Rolston, D. E. (2010). The gas-diffusivity-based Buckingham tortuosity factor from pF 1 to 6.91 as a soil structure fingerprint. In *Proceedings of the 19th World Congress of Soil Science: Soil solutions for a changing world, Brisbane, Australia, 1-6 August 2010.* (pp. 76-79).

Dexter, A. R. (1997). Physical properties of tilled soils. *Soil and Tillage Research*, *43*(1), 41-63.

Dexter, A. R. (2004). Soil physical quality: Part I. Theory, effects of soil texture, density, and organic matter, and effects on root growth. *Geoderma*, *120*(3), 201-214.

Dexter, A. R., Richard, G., Arrouays, D., Czyż, E. A., Jolivet, C., & Duval, O. (2008). Complexed organic matter controls soil physical properties. *Geoderma*, *144*(3), 620-627.

Dogan, A. U., Dogan, M., Onal, M., Sarikaya, Y., Aburub, A., & Wurster, D. E. (2006). Baseline studies of the clay minerals society source clays: specific surface area by the Brunauer Emmett Teller (BET) method. *Clays and Clay Minerals*, *54*(1), 62-66.

Dorner, J., Sandoval, P., & Dec, D. (2010). The role of soil structure on the pore functionality of an ultisol. *Journal of soil science and plant nutrition*, *10*(4), 495-508.

Eggleston, J. R., & Peirce, J. J. (1995). Dynamic programming analysis of pore space. *European journal of soil science*, *46*(4), 581-590.

Elliot, T. R., Reynolds, W. D., & Heck, R. J. (2010). Use of existing pore models and X-ray computed tomography to predict saturated soil hydraulic conductivity. *Geoderma*, *156*(3), 133-142.

Ersahin, S., Gunal, H., Kutlu, T., Yetgin, B., &Coban, S. (2006). Estimating specific surface area and cation exchange capacity in soils using fractal dimension of particle-size distribution. *Geoderma*, *136*(3), 588-597.

Feldkamp, L. A., Davis, L. C., & Kress, J. W. (1984). Practical cone-beam algorithm. *The Journal of the Optical Society of America A*, *1*(6), 612-619.

Gahoonia, T. S., Care, D., & Nielsen, N. E. (1997). Root hairs and phosphorus acquisition of wheat and barley cultivars. *Plant and Soil*, *191*(2), 181-188.

Gaiser, T., Perkons, U., Küpper, P. M., Puschmann, D. U., Peth, S., Kautz, T., ... & Köpke, U. (2012). Evidence of improved water uptake from subsoil by spring wheat following lucerne in a temperate humid climate. *Field Crops Research*, *126*, 56-62.

Garbout, A., Munkholm, L. J., & Hansen, S. B. (2013). Tillage effects on topsoil structural quality assessed using X-ray CT, soil cores and visual soil evaluation. *Soil and Tillage Research*, *128*, 104-109.

Garbout, A., Munkholm, L. J., Hansen, S. B., Petersen, B. M., Munk, O. L., & Pajor, R. (2012). The use of PET/CT scanning technique for 3D visualization and quantification of real-time soil/plant interactions. *Plant and soil*, *352*(1-2), 113-127.

Gerke, H. H., Dusek, J., & Vogel, T. (2013). Solute mass transfer effects in two-dimensional dual-permeability modeling of bromide leaching from a tile-drained field. *Vadose Zone Journal*, *12*.

Glinkski, J., &Stepniewski, W. (1985). *Soil aeration and its role for plants*. United States, Florida, Boca Raton: CRC Press.

Gregory, A. S., Bird, N. R., Whalley, W. R., Matthews, G. P., & Young, I. M. (2010). Deformation and shrinkage effects on the soil water release characteristic. *Soil Science Society of America Journal*, *74*(4), 1104-1112.

Gregory, P.J. (2008). *Plant Roots: Growth, Activity and Interactions with the Soil*. United Kingdom, Oxford: Blackwell Publishing Ltd.

Hajnos, M., Korsunskaia, L., &Pachepsky, Y. (2000). Soil pore surface properties in managed grasslands. *Soil and Tillage Research*, *55*(1), 63-70.

Hayes, R. C., Li, G. D., Dear, B. S., Conyers, M. K., Virgona, J. M., & Tidd, J. (2010). Perennial pastures for recharge control in temperate drought-prone environments. Part 2: soil drying capacity of key species. *New Zealand Journal of Agricultural Research*, *53*(4), 327-345.

Horgan, G. W. (1999). An investigation of the geometric influences on pore space diffusion. *Geoderma*, *88*(1), 55-71.

Horn, R., Domzzal, H., Slowinska-Jurkiewicz, A., & Van Ouwerkerk, C. (1995). Soil compaction processes and their effects on the structure of arable soils and the environment. *Soil and Tillage Research*, *35*(1), 23-36.

IUSS Working Group WRB. (2006). *World reference base for soil resources 2006: A framework for international classification, correlation and communication*. *Word Soil Resources Report No. 103.* Rome: FAO.

Iversen, B. V., Børgesen, C. D., Lægdsmand, M., Greve, M. H., Heckrath, G., & Kjærgaard, C. (2011). Risk predicting of macropore flow using pedotransfer functions, textural maps, and modeling. *Vadose Zone Journal*, *10*(4), 1185-1195.

Kadžienė, G., Munkholm, L. J., &Mutegi, J. K. (2011). Root growth conditions in the topsoil as affected by tillage intensity. *Geoderma*, *166*(1), 66-73.

Kaestner, A., Schneebeli, M., & Graf, F. (2006). Visualizing three-dimensional root networks using computed tomography. *Geoderma*, *136*(1), 459-469.

Kautz, T., Amelung, W., Ewert, F., Gaiser, T., Horn, R., Jahn, R., ... & Köpke, U. (2012). Nutrient acquisition from arable subsoils in temperate climates: A review. *Soil Biology and Biochemistry*, *57*, 1003-1022.

Kautz, T., Landgraf, D., & Köpke, U. (2011). *Proceedings of the 3rd Scientific Conference*. Gyeonggi Paldang, Republic of Korea.

Kautz, T., & Köpke, U. (2010). In situ endoscopy: New insights to root growth in biopores. *Plant Biosystems*, *144*(2), 440-442.

Kawamoto, K., Moldrup, P., Schjønning, P., Iversen, B. V., Rolston, D. E., & Komatsu, T. (2006). Gas Transport Parameters in the Vadose Zone. *Vadose Zone Journal*, *5*(4), 1194-1204.

Kristensen, A. H., Thorbjørn, A., Jensen, M. P., Pedersen, M., &Moldrup, P. (2010). Gas-phase diffusivity and tortuosity of structured soils. *Journal of contaminant hydrology*, *115*(1), 26-33.

Kutschera, L., Lichtenegger, E., & Sobotik, M. (2009). *Wurzelatlas der Kulturpflanzen gemäßigter Gebiete: mit Arten des Feldgemüsebaues*. DLG-Verlag GmbH, Deutschland, Frankfurt.

Liang, J., Zhang, J., & Wong, M. H. (1996). Effects of air-filled soil porosity and aeration on the initiation and growth of secondary roots of maize (Zea mays). *Plant and Soil*, *186*(2), 245-254.

Lindquist, W.B., Lee, S.-M., Coker, D.A., Jones, K.W., & Spanne, P. (1995). *Medial Axis Analysis of Three Dimensional Tomographic Images of Drill Core Samples*. SUNY-Stony Brook technical report SUNYSB-AMS-95-01.

Lindquist, W. B., Venkatarangan, A., Dunsmuir, J., & Wong, T. F. (2000). Pore and throat size distributions measured from synchrotron X‐ray tomographic images of Fontainebleau sandstones. *Journal of Geophysical Research: Solid Earth (1978–2012)*, *105*(B9), 21509-21527.

Lipiec, J., & Hatano, R. (2003). Quantification of compaction effects on soil physical properties and crop growth. *Geoderma*, *116*(1), 107-136.

Mairhofer, S., Zappala, S., Tracy, S. R., Sturrock, C., Bennett, M., Mooney, S. J., & Pridmore, T. (2012). RooTrak: Automated recovery of three-dimensional plant root architecture in soil from X-Ray microcomputed tomography images using visual tracking. *Plant physiology*, *158*(2), 561-569.

Mairhofer, S., Zappala, S., Tracy, S., Sturrock, C., Bennett, M. J., Mooney, S. J., & Pridmore, T. P. (2013). Recovering complete plant root system architectures from soil via X-ray µ-Computed Tomography. *Plant methods*, *9*(8), 1-7.

Marshall, T. J. (1959). The diffusion of gases through porous media. *Journal of Soil Science*, *10*(1), 79-82.

Matthews, G. P., Laudone, G. M., Gregory, A. S., Bird, N. R. A., Matthews, A. G., & Whalley, W. R. (2010). Measurement and simulation of the effect of compaction on the pore structure and saturated hydraulic conductivity of grassland and arable soil. *Water Resources Research*, *46*(5).

McKenzie, B. M., Bengough, A. G., Hallett, P. D., Thomas, W. T. B., Forster, B., & McNicol, J. W. (2009). Deep rooting and drought screening of cereal crops: A novel field-based method and its application. *Field Crops Research*, *112*(2), 165-171.

Meek, B. D., Rechel, E. A., Carter, L. M., & DeTar, W. R. (1989). Changes in infiltration under alfalfa as influenced by time and wheel traffic. *Soil Science Society of America Journal*, *53*(1), 238-241.

Millington, R. J. (1959). Gas diffusion in porous media. *Science*, *130*, 100-102.

Mitchell, A. R., Ellsworth, T. R., & Meek, B. D. (1995). Effect of root systems on preferential flow in swelling soil. *Communications in Soil Science & Plant Analysis*, *26*(15-16), 2655-2666.

Moldrup, P., Olesen, T., Komatsu, T., Schjønning, P., & Rolston, D. E. (2001). Tortuosity, diffusivity, and permeability in the soil liquid and gaseous phases. *Soil Science Society of America Journal*, *65*(3), 613-623.

Moldrup, P., Poulsen, T. G., Schjønning, P., Olesen, T., & Yamaguchi, T. (1998). Gas permeability in undisturbed soils:

Measurements and predictive models. *Soil Science*, *163*(3), 180-189.

Mooney, S. J. (2002). Three-dimensional visualization and quantification of soil macroporosity and water flow patterns using computed tomography. *Soil Use and Management*, *18*(2), 142-151.

Naveed, M., Moldrup, P., Arthur, E., Wildenschild, D., Eden, M., Lamandé, M., ... & de Jonge, L. W. (2013). Revealing soil structure and functional macroporosity along a clay gradient using X-Ray Computed Tomography. *Soil Science Society of America Journal*, *77*(2), 403-411.

Nye, P. H. (1994). The effect of root shrinkage on soil water inflow. *Philosophical Transactions of the Royal Society of London. Series B: Biological Sciences*, *345*, 395-402.

Oh, W., & Lindquist, W. B. (1999). Image thresholding by indicator kriging. *IEEE Transactions onPattern Analysis and Machine Intelligence, 21*(7), 590-602.

Pagenkemper, S. K., Peth, S., Puschmann, D. U., & Horn, R. (2013). Effects of root-induced biopore architectures on physical processes investigated with industrial X-Ray Computed Tomography. In Anderson, S. H., Hopmans, J. W. (Eds.), *Soil–Water–Root Processes: Advances in Tomography and Imaging* (pp. 67-94). SSSA Special Publication 61. 2013. United States, Wisconsin, Madison.

Pagenkemper, S.K., Athmann, M., Puschmann, D. U., Kautz, T., Peth, S., & Horn, R. (2014). The effect of earthworm activity on soil bioporosity—Investigated with X-ray computed tomography and endoscopy. *Soil and Tillage Research* (*in press*). doi: 10. 1016/j.still.2014.05.007

Paul, J. L., & Lee, C. I. (1976). Relation between growth of Chrysanthemum and aeration of various container media. *Journal of the American Society for Horticultural Science, 101*, 500–503.

Peth, S., Horn, R., Beckmann, F., Donath, T., Fischer, J., & Smucker, A. J. M. (2008). Three-dimensional quantification of intra-aggregate pore-space features using synchrotron-radiation-based microtomography. *Soil Science Society of America Journal*, *72*(4), 897-907.

Pietola, L. M., & Smucker, A. J. (1995). Fine root dynamics of alfalfa after multiple cuttings and during a late invasion by weeds. *Agronomy Journal*, *87*(6), 1161-1169.

R Development Core Team.(2011). *R: A language and environment for statistical computing, R Foundation for statistical computing*. Ed. Vienna, Austria.

Rasse, D. P., & Smucker, A. J. (1998). Root recolonization of previous root channels in corn and alfalfa rotations. *Plant and Soil*, *204*(2), 203-212.

Schäffer, B., Stauber, M., Müller, R., & Schulin, R. (2007). Changes in the macro‐pore structure of restored soil caused by compaction beneath heavy agricultural machinery: A morphometric study. *European Journal of Soil Science*, *58*(5), 1062-1073.

Schlüter, S., Vogel, H. J., Ippisch, O., Bastian, P., Roth, K., Schelle, H., ... & Vanderborght, J. (2012). Virtual soils: Assessment of the effects of soil structure on the hydraulic behavior of cultivated soils. *Vadose Zone Journal*, *11*(4).

Schmidt, S., Bengough, A. G., Gregory, P. J., Grinev, D. V., & Otten, W. (2012). Estimating root–soil contact from 3D X‐ray microtomographs. *European Journal of Soil Science*, *63*(6), 776-786.

Schroetter, S., Rogasik, J., & Schnug, E. (2007). Root Growth and Agricultural Management. In *Encyclopedia of Soil Science, Second Edition* (pp. 1531–1534). United Kingdom, London: Taylor & Francis.

Taina, I. A., Heck, R. J., & Elliot, T. R. (2008). Application of X-ray computed tomography to soil science: A literature review. *Canadian Journal of Soil Science*, *88*(1), 1-19.

Tinker, P. B. (1976). Transport of water to plant roots in soil. *Philosophical Transactions of the Royal Society of London. B, Biological Sciences*, *273*, 445-461.

Tracy, S. R., Roberts, J. A., Black, C. R., McNeill, A., Davidson, R., & Mooney, S. J. (2010). The X-factor: Visualizing undisturbed root architecture in soils using X-ray computed tomography. *Journal of experimental botany*, *61*(2), 311-313.

Uteau, D., Pagenkemper, S. K., Peth, S., & Horn, R. (2013). Root and time dependent soil structure formation and its influence on gas transport in the subsoil. *Soil and Tillage Research*, *132*, 69-76.

Vogel, H. J., Weller, U., & Schlüter, S. (2010). Quantification of soil structure based on Minkowski functions. *Computers & Geosciences*, *36*(10), 1236-1245.

Wojdyr, M. (2010). Fityk: A general-purpose peak fitting program. *Journal of Applied Crystallography*, *43*(5), 1126-1128.